

PAPER • OPEN ACCESS

Spatial and temporal pulse shaping for lateral and depth resolved two-photon excited fluorescence contrast

To cite this article: A Kussicke *et al* 2020 *J. Phys. B: At. Mol. Opt. Phys.* **53** 025401

View the [article online](#) for updates and enhancements.



IOP | ebooks™

Bringing you innovative digital publishing with leading voices to create your essential collection of books in STEM research.

Start exploring the collection - download the first chapter of every title for free.

Spatial and temporal pulse shaping for lateral and depth resolved two-photon excited fluorescence contrast

A Kussicke, M Tegtmeier, F Büchau, K Heyne and A Lindinger 

Institut für Experimentalphysik, Freie Universität Berlin, Arnimallee 14, D-14195, Berlin, Germany

E-mail: lindin@physik.fu-berlin.de

Received 6 June 2019, revised 2 October 2019

Accepted for publication 13 November 2019

Published 18 December 2019



CrossMark

Abstract

We report combined temporal and spatial laser pulse shaping to perform lateral and depth dependent two-photon excited fluorescence of dyes. For generating the specific spatially and temporally phase tailored pulses a temporal pulse shaper and a subsequent spatial pulse shaper are employed. Simultaneous spatial and temporal shaping is presented for two-photon excited fluorescence by applying temporal third order phase functions on spatially different light field components. Moreover, the prospects of spatial shaping are demonstrated by applying various lateral two-photon fluorescence pattern. In particular, a depth dependent excitation of different dyes is performed which leads to a high axially resolved fluorescence contrast. The introduced spatial and temporal shaping technique provides new perspectives for biophotonic imaging applications.

Keywords: pulse shaping, spatial beam modification, two-photon excited fluorescence

(Some figures may appear in colour only in the online journal)

1. Introduction

In the last years laser pulse shaping has become a powerful and versatile tool in several research fields (e.g. [1–6]). For this purpose, Fourier domain shaping with liquid crystal modulators is employed which leads to temporally tailored light fields. This allows for controlling molecular processes with temporally shaped pulses in order to achieve a pre-defined target state [7–9]. Moreover, modification of the light polarization was additionally included to extend the pulse shaping feasibilities [10]. Laser pulse shaping is particularly applied for multiphoton excited fluorescence where intrapulse interference is utilized to selectively address different molecules [11]. This is most useful for three-dimensional imaging in multiphoton microscopy [12].

Similar to the temporal shaping it is also possible to modify the spatial laser profile by using focussing lenses and a two dimensional liquid crystal array combined to a spatial light shaper [13, 14]. This wavefront shaping technique leads to definable tailored beam profiles in the focal plane. Shaped spatial beam profiles were applied for high resolved spatial imaging [15, 16], microstructuring [17], and deep tissue focussing [18]. Modifying the focal depth by employing specific spatial phase pattern allows for deep layer imaging by two-photon excited fluorescence microscopy [19]. First approaches were already undertaken to combine temporal and spatial shaping techniques [20–23]. Simultaneous temporal and spatial pulse shaping has a high scientific potential since it enables for controlling fundamental photo-induced processes concurrently temporally and spatially.

This contribution is concerned with simultaneous temporal and spatial pulse shaping to generate user defined pulses which are employed for two-photon excited fluorescence. These experiments are performed with a recently developed pulse shaper setup consisting of a temporal and a subsequent spatial shaper. It allows for simultaneous and independent



Original content from this work may be used under the terms of the [Creative Commons Attribution 3.0 licence](https://creativecommons.org/licenses/by/3.0/). Any further distribution of this work must maintain attribution to the author(s) and the title of the work, journal citation and DOI.

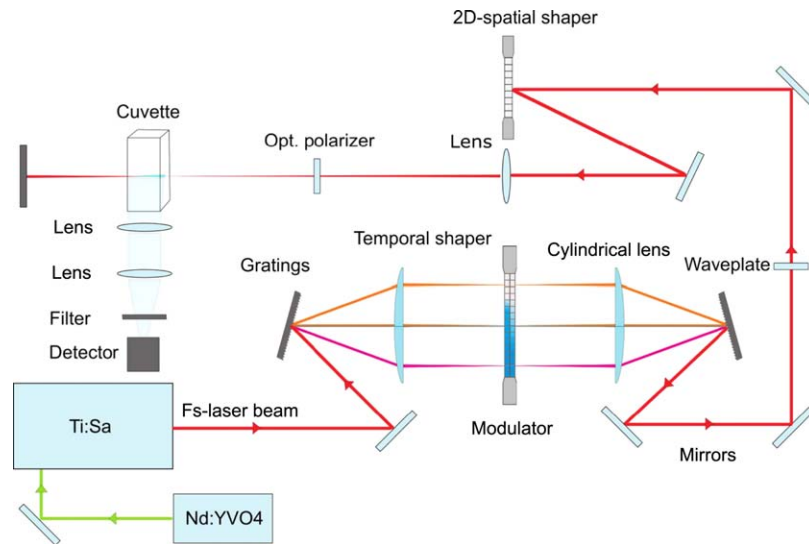


Figure 1. Schematic experimental setup with a fs-laser (Ti:Sa), a temporal pulse shaper with gratings and a liquid crystal light modulator, a half-wave plate for turning the light polarization, and a spatial beam shaper with a 2D liquid crystal array. Furthermore, a cuvette for fluorescence excitation and optical components for detection are shown. The laser beam first passes the temporal pulse shaper, then its polarization is turned to optimally pass the spatial pulse shaper, and finally the modulated beam is focused into a cuvette. The induced fluorescence is directed into a fiber spectrometer by using two collecting lenses. The detection is either parallel or perpendicular to the laser beam direction.

temporal shaping of different spatial components. Contrasts are received by using antisymmetric third order phase functions for temporal shaping. Lateral pulse shaping is presented for parallel and perpendicular fluorescence detection geometry. In particular, the combined shaping method is applied to first establish depth dependent selective excitation of different dyes, which leads to a high axially resolved fluorescence contrast. These optical tools will be relevant for biophotonic imaging.

2. Experimental

The scheme of the experimental setup is displayed in figure 1. A frequency-doubled Nd:YVO₄ laser (Verdi V, Coherent, Inc.) pumps a broadband titanium sapphire laser oscillator (Femtosecond Compact, Femtolasers), having an average power of 350 mW with a repetition rate of 75 MHz. The central wavelength is adjusted to 805 nm with a spectral full width at half maximum of about 80 nm. The ultrashort laser pulses pass a 4f pulse shaper with a computer controlled liquid crystal light modulator (SLM 640, Cambridge Research Instruments). This allows for independently shaping the phase and polarization of the light field. The temporally modified laser pulses are subsequently guided to the spatial modulator (PLUTO-NIR-015-C, HOLOEYE Photonics AG). The spatial shaper for forming the spatial laser profile consists of a 2D array with 1920 × 1080 liquid crystal elements and a reflective surface behind. The display exhibits an active area of 15.36 mm × 8.64 mm. A focussing lens ($f = 300$ mm) is placed 300 mm behind the 2D modulator and the spatially shaped focal profile can be detected by a camera (AW335, Ausdom Inc.). Polarizer, waveplate and filter are utilized for shaping and signal detection. With the temporal shaper the spectral phases are independently modulated

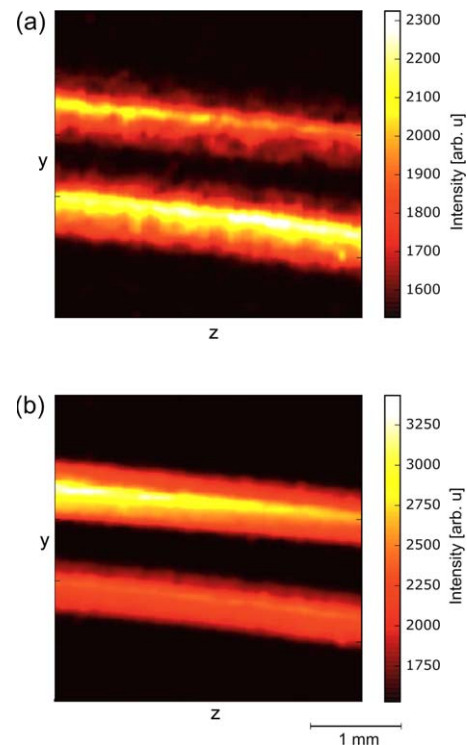


Figure 2. Images of the fluorescence intensities in a cuvette induced by spatially separated phase shaped polarization components perpendicular to the beam. (a) Fluorescence image of cumarin 102 for the third order phase shaped vertical polarization component at $\lambda_0 = 820$ nm (upper trace) and the third order phase shaped horizontal component at $\lambda_0 = 780$ nm (lower trace). (b) Corresponding figure for rhodamine B. The spatially separated pulse components show differing fluorescence intensities, which allows for predominant excitation of one dye by one pulse component and simultaneously the other dye by the other spatially shifted component.

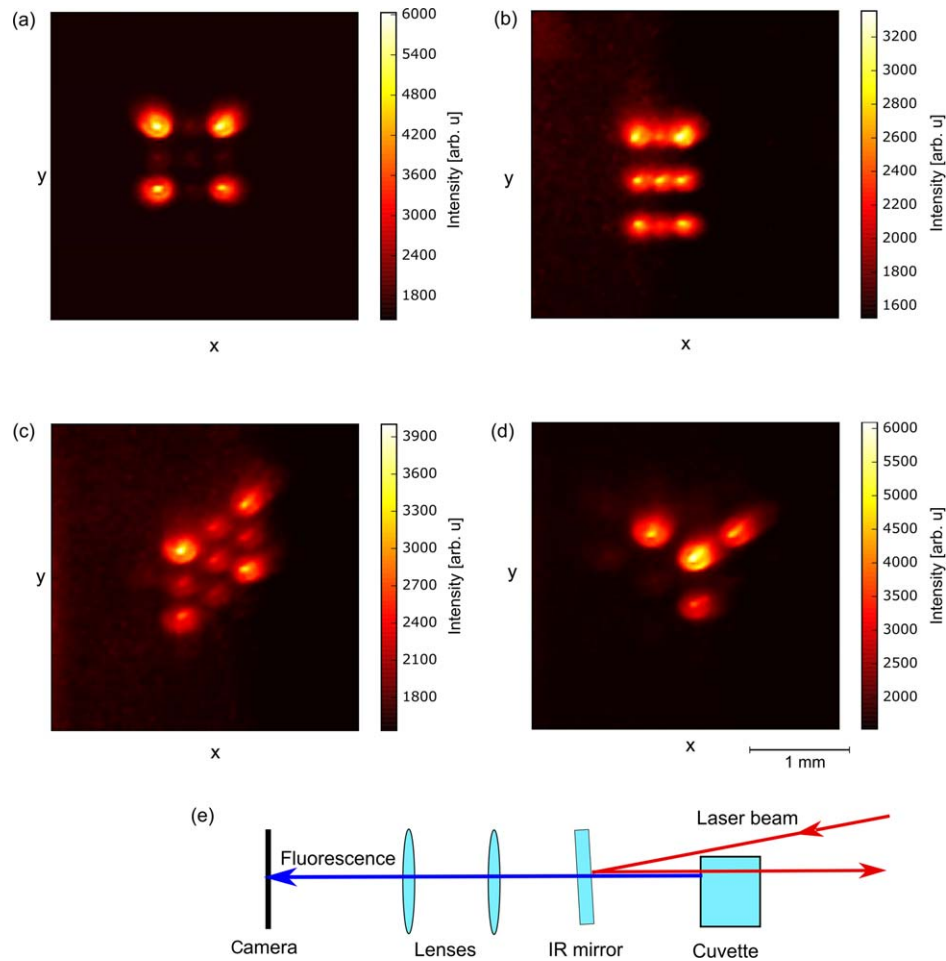


Figure 3. Rhodamin B fluorescence intensities in a cuvette excited by spatially tailored laser pulses, recorded in top view detection geometry. The laterally separated pulse components show differing fluorescence intensity profiles. (a) Square shaped spot pattern generated by perpendicularly crossed sinusoidal gratings with periods of 70 pixel. (b) Rectangular spot pattern produced by perpendicularly crossed sinusoidal gratings with different periods of 50 pixel and 100 pixel. (c) Rhombic spot pattern produced by sinusoidal gratings with an angle of 45° in between. (d) Triangular spot pattern generated by three sinusoidal gratings with angles of 60° in between. (e) Detection scheme for top view detection of the two-photon fluorescence.

on the two polarization axes at $\pm 45^\circ$ to the horizontal. For rotating the polarization a $\lambda/2$ -waveplate is inserted which turns the temporally shaped polarization components to the vertical and horizontal direction. Thus, they are projected on the vertical and horizontal axes of the 2D array to allow for different spatial profiles of these components. With this configuration of the experimental setup, the horizontal polarization component can be spatially shaped while the vertical polarization component will remain as a Gaussian-profile for all measurements. In some measurements the vertically polarized component is removed by a polarizer.

In order to perform the fluorescence experiments, after the shaper the beam is directed into a quartz glass cuvette with the dyes solvated in ethanol. A further short focal length lens (30 or 50 mm) is located close to the cuvette in order to create a stronger focus. The dyes rhodamine B (*rhoB*) and coumarin 102 (*c102*) were employed for two-photon excitations because they exhibit high quantum yields [24, 25]. The fluorescence detection is either parallel or perpendicular to the laser beam direction. For perpendicular fluorescence detection, the laser beam waist was placed close to the inner side

glass wall for minimizing self-absorption and hence to acquire the maximal fluorescence signal. The emitted light is focused by two lenses into the recording camera and a glass filter (BG 39) is used to reduce the stray light of the laser. For finding transform-limited pulses an optimization by phase resolved interferometric spectral modulation [26] was performed in order to receive the phase retardances.

3. Results

3.1. Lateral pulse shaping

The initial experiments were conducted for perpendicular fluorescence detection. Figure 2 shows camera images of the fluorescence intensities in a cuvette induced by spatially separated phase shaped polarization components. The upper traces display the two-photon fluorescence of coumarin 102 and rhodamine B for the third order phase shaped vertical polarization component at $\lambda_0 = 820$ nm and the lower traces show the third order phase shaped horizontal component at

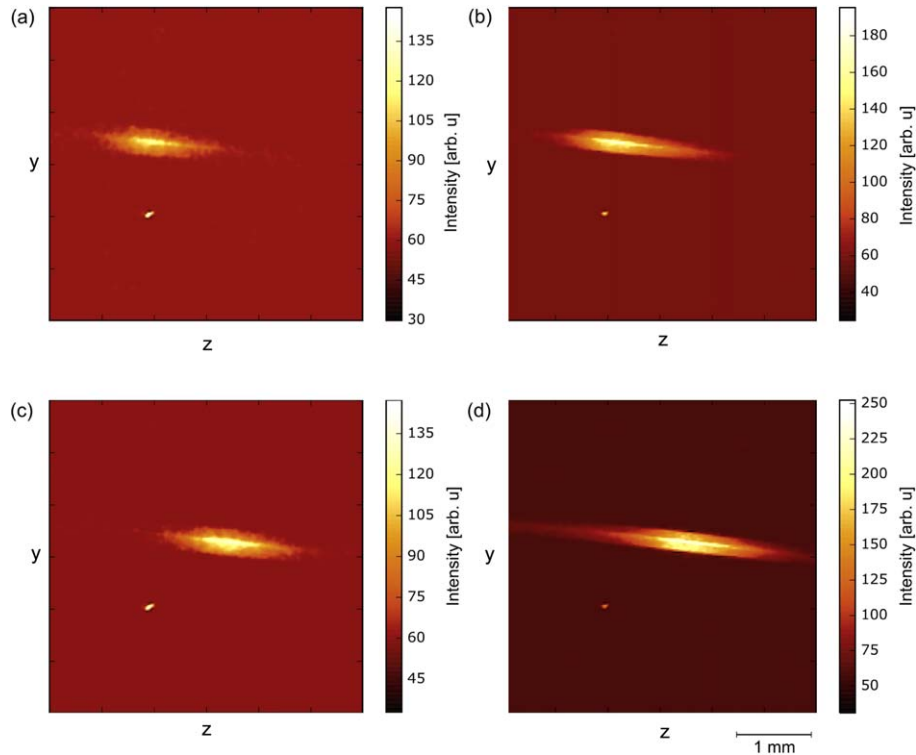


Figure 4. Depth dependent spatial pulse shaping. Zernike polynomials are applied on the 2D array in order to shift the two-photon excited fluorescence focal spot. (a) and (c) display the images of the Zernike polynomial Z_0^2 with a prefactor of -80 and (b) and (d) the images of the polynomial Z_0^2 with a prefactor of -150 for coumarin and rhodamine B, respectively. A clear spatial depth shift is observed for both dyes.

$\lambda_0 = 780$ nm, respectively. The horizontal polarization component is vertically downshifted by applying a linear spatial phase using the Zernike polynomial Z_1^{-1} with a factor of 170 inscribed on the 2D array of the spatial pulse shaper. The spatially separated pulse components exhibit differing two-photon induced fluorescence intensities due to their specific spectral phase functions. This enables for predominant excitation of one dye by one spatial pulse component and simultaneously for excitation of the other dye by the other spatial component. In particular, the upper trace optimizes the two-photon fluorescence of rhodamine B and the lower trace the fluorescence of coumarin 102, whereby rhodamine B is generally more intense than coumarin 102.

The second measurement is performed for top view detection of the fluorescence, whereby the detector faces the surface of the cuvette. To this end, a dielectric reflecting mirror is inserted to direct the beam on the surface of the cuvette with the fluorescence light transmitting the mirror. This top view geometry allows for simultaneous excitation and detection on the surface normal. For this case, the not spatially modified vertically polarized pulse component is removed by inserting a polarizer. The temporal phase is set to a constant value to get a short pulse for receiving maximal fluorescence signal. Figure 3 presents the images of the cuvette with rhodamine B. Sinusoidal phase gratings $\phi(p) = A \sin(2\pi p/\lambda)$ were written on the modulator, with the amplitude A , the liquid crystal element number p , and the period λ . Any two-photon excitation pattern can be realized by applying the suitable 2D phase functions on the spatial

modulator. It has to be noted that the two-photon fluorescence intensities depend on the square of the light intensities. Hence, mainly the high intense light components will be visible in the image.

3.2. Depth resolved pulse shaping

For deep tissue imaging applications it is highly relevant to perform axially resolved two-photon excited fluorescence measurements. With the presented setup it is feasible to additionally modify the focal depth by inscribing appropriate 2D phase functions on the spatial modulator. Also in this case the vertically polarized pulse component is removed by a polarizer. Figure 4 displays fluorescence images recorded by inserting Zernike polynomials on the 2D array in order to shift the two-photon excited fluorescence focal spot in beam direction. Figures 4(a) and (c) show the images of the Zernike polynomial Z_0^2 with a prefactor of -80 and figures 4(b) and (d) the images with a prefactor of -150 for coumarin and rhodamine B, respectively. A clear spatial depth shift is observed for both dyes.

Figure 5 shows the spatial depth dependent contrast. For that purpose, the contrast values are plotted over the distance in z -direction corresponding to the beam axis. The graph depicts the added contrasts at the two focal distances with the prefactors -80 and -150 of the Zernike polynomial Z_0^2 inscribed on the 2D array of the modulator. A clear contrast difference of about 0.1 is obtained at an axial distance of approximately 0.4 mm.

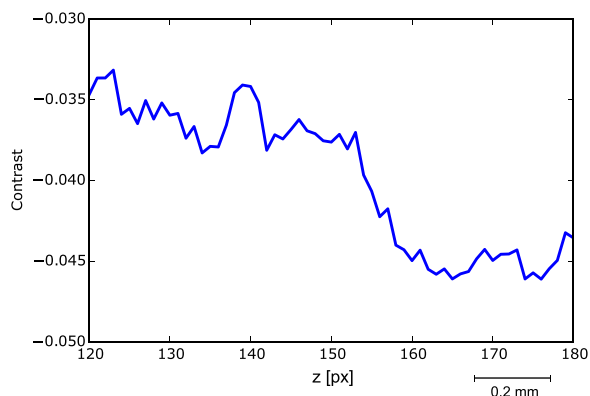


Figure 5. Spatial depth dependent contrast. The curve displays the added contrasts at the two focal distances with the prefactors -80 and -150 of the Zernike polynomial Z_0^2 inscribed on the 2D array. A distinct contrast difference of 0.1 is obtained at an axial distance of about 0.4 mm.

4. Conclusion

A spatially resolved two-photon excited fluorescence contrast was obtained by simultaneous and combined temporal and spatial laser pulse shaping. To that end, a temporal pulse shaper and a subsequent spatial pulse shaper were utilized to design the specific spatially and temporally phase tailored pulses. Laterally modulated two-photon excitation of different dyes by applying temporal third order phase functions was demonstrated for different excitation and detection geometries. Particularly, spatial pulse shaping was additionally employed for depth dependent excitation and a considerable axially resolved fluorescence contrast was measured. This novel approach could be employed for improved contrast recordings of autofluorescing molecules. The described spatial and temporal shaping method allows for simultaneous measurements at different spatial positions with well controllable light fields which will lead to novel biophotonic applications.

Acknowledgments

The Klaus Tschira Foundation (KTS) is acknowledged for financial support (project 00.314.2017).

ORCID iDs

A Lindinger  <https://orcid.org/0000-0002-1494-645X>

References

- [1] Assion A, Baumert T, Bergt M, Brixner T, Kiefer B, Seyfried V, Strehle M and Gerber G 1998 *Science* **282** 919–22
- [2] Brixner T and Gerber G 2003 *Chem. Phys. Chem.* **4** 418–38
- [3] Vogt G, Krampert G, Niklaus P, Nuernberger P and Gerber G 2005 *Phys. Rev. Lett.* **94** 068305
- [4] Aeschlimann M, Bauer M, Bayer D, Brixner T, Garcia de Abajo F J, Pfeiffer W, Rohmer M, Spindler C and Steeb F 2007 *Nature* **446** 301–4
- [5] Lindinger A, Lupulescu C, Plewicky M, Vetter F, Merli A, Weber S M and Wöste L 2004 *Phys. Rev. Lett.* **93** 033001
- [6] Wohlleben W, Buckup T, Herek J L and Motzkus M 2005 *Chem. Phys. Chem.* **6** 850–7
- [7] Judson R S and Rabitz H 1992 *Phys. Rev. Lett.* **68** 1500–3
- [8] Nuernberger P, Vogt G, Brixner T and Gerber G 2007 *Phys. Chem. Chem. Phys.* **9** 2470–97
- [9] Dantus M and Lozovoy V V 2004 *Chem. Rev.* **104** 1813–60
- [10] Weise F and Lindinger A 2010 *Appl. Phys. B* **101** 79–91
- [11] Lozovoy V V, Pastirk I, Walowicz K A and Dantus M 2002 *J. Chem. Phys.* **118** 3187–96
- [12] Denk W, Strickler J H and Webb W W 1990 *Science* **248** 73–6
- [13] Sanner N, Huot N, Audouard E, Larat C and Huignard J-P 2005 *Opt. Lett.* **30** 1479–81
- [14] Maurer C, Jesacher A, Bernet S and Ritsch-Marte M 2011 *Laser Photonics Rev.* **5** 81–101
- [15] Hell S and Wichmann J 1994 *Opt. Lett.* **19** 780–2
- [16] Moneron G and Hell S 2009 *Opt. Exp.* **17** 14567–73
- [17] Sanner N, Huot N, Audouard E, Larat C and Huignard J-P 2007 *Opt. Lasers Eng.* **45** 737–41
- [18] Tanabe A, Hibi T, Ipponjima S, Matsumoto K, Yokoyama M, Kurihara M, Hashimoto N and Nemoto T 2015 *J. Biomed. Opt.* **20** 101204
- [19] Perry S, Burke R and Brown E 2012 *Ann. Biomed. Eng.* **40** 277
- [20] Feurer T, Vaughan J C, Koehl R M and Nelson K A 2002 *Opt. Lett.* **27** 652–4
- [21] McCabe D J, Tajalli A, Austin D R, Bondareff P, Walmsley I A, Gigan S and Chatel B 2011 *Nat. Commun.* **2** 447
- [22] Katz O, Small E, Bromberg Y and Silberberg Y 2011 *Nat. Photon.* **5** 372–7
- [23] Feurer T, Vaughan J C and Nelson K A 2003 *Science* **299** 374–7
- [24] Snare M J, Treloar F, Ghiggino K P and Thistlethwaite P J 1982 *J. Photochem.* **18** 335–46
- [25] Kubin R F and Fletcher A N 1982 *J. Luminescence* **27** 455–62
- [26] Wu T, Tang J, Hajj B and Cui M 2011 *Opt. Express* **19** 12961